from right to left at a velocity v_1 for a time $T_1 = ma/v_1$ (where m is some large integer). We then imagine the motion to be reversed at a different velocity v_2 for a time $T_2 = ma/v_2$. The situation at the end of these two successive motions is identical to that at the beginning. The total amount of flux linking a loop contour taken within the superconductors and passing through the junction at two points must be the same at the beginning and end. It follows again from Faraday's law that Γ must be independent of velocity, and hence of voltage or frequency.

In summary, it seems that any deviations of the Josephson voltage-frequency ratio from nonexotic sources can only occur if Faraday's law is incorrect.

[1]J. Clarke, Phys. Rev. Lett. **21,** 1566 (1968).
[2]T. F. Finnegan, A. Denenstein, and D. N. Langenberg, Phys. Rev. B **4,** 1487 (1971).
[3]T. D. Bracken and W. D. Hamilton, Phys. Rev. B **6,** 2603 (1972).
[4]D. N. Langenberg, W. H. Parker, and B. N. Taylor, Phys. Rev. **150,** 186 (1966); W. H. Parker, B. N. Taylor, and D. N. Langenberg, Phys. Rev. Lett. **18,** 287 (1967). See also Ref. 2 for a more complete list of references.
[5]F. Bloch, Phys. Rev. Lett. **21,** 1241 (1968); Phys. Rev. B **2,** 109 (1970).
[6]B. D. Josephson, Adv. Phys. **14,** 419 (1965).
[7]P. W. Anderson, in *Progress in Low-Temperature Physics,* edited by C. J. Gorter (North-Holland, Amsterdam, 1967), Vol. 5, p. 1.
[8]P. Lebwohl and M. J. Stephen, Phys. Rev. **163,** 376 (1967); A. C. Scott, Bull. Am. Phys. Soc. **12,** 308 (1967); A. C. Scott, Am. J. Phys. **37,** 52 (1969).

PHYSICAL REVIEW B VOLUME 7, NUMBER 3 1 FEBRUARY 1973

Microwave Surface Resistance of Type-II Superconductors in the Vortex State*

R. J. Pedersen
Aerospace Corporation, El Segundo, California 90245
and
Y. B. Kim and R. S. Thompson
University of Southern California, Los Angeles, California 90007
(Received 20 July 1972)

We have measured the microwave surface resistance of various Nb-Ta and Pb-In superconducting alloys using a derivative technique to determine its rate of change with field near H_{c2}. Previous dc measurements of this slope have generally been interpreted to show agreement with the Caroli–Maki theory, which Thompson has found to be incomplete. Our measurements show a region of constant slope somewhat below H_{c2} with a magnitude in agreement with the dc results, but also show that the slope increases rapidly to approach the Thompson values in the limit $H \to H_{c2}$. Theoretical arguments are presented indicating why the two theories can have different regions of validity.

I. INTRODUCTION

In recent years, some controversy has developed concerning predictions of various microscopic developments of the theory of type-II superconductors. One area of particular interest is the discontinuity in slope of the flux-flow resistance of "dirty" disordered alloys at H_{c2}, the upper critical magnetic field. Theoretical calculation in this limit is greatly simplified since all quantities in the microscopic theory may be expanded in powers of the order parameter, which is not the case either for lower fields or in general for "clean" well-ordered crystals.

Application of the time-dependent Ginzburg–Landau theory to the flux-flow phenomenon was first attempted by Schmid.[1] Near T_c, he calculated the slope of flux-flow resistivity variation in H in the limit of $H \to H_{c2}$ and compared the results with the original flux-flow data obtained by Kim *et al.*[2] Subsequently, Caroli and Maki[3] generalized Schmid's theory to all temperatures, and numerous experimental results on flux flow have been compared with the Caroli–Maki calculation. Prior to this work, Caroli and Maki[4] had proposed a theory of the time-dependent fluctuations of the order parameter which is also capable of yielding the flux-flow resistivity. While this first theory of Caroli and Maki represents an approach quite different from that of Schmid, it predicts an infinite dc conductivity in contradiction to all experimental observations on flux flow. Later, Thompson[5] found both theories of Caroli and Maki incomplete and calculated the additional contributions which should be added to each theory to obtain a new consistent result from both approaches. The necessity of Thompson's corrections to the Caroli–Maki theories has also been verified by Takayama and Eb-

isawa.[6] Henceforth, we will ignore the first Caroli–Maki theory and only refer to the second one, which is useful for comparison with experiment.

The contribution of Thompson's correction term increases from zero monotonically with the temperature; at T_c it equals the Caroli–Maki terms, thus doubling the slope of flux-flow resistivity at H_{c2}. Although a number of experiments have been performed in various laboratories, so far the spread in data has been too great to strongly support one theory over another. The circumstance leading to this situation was reviewed by one of the present authors.[7] In general, the observed resistance slope near H_{c2} is a strongly varying function of field, and thus a considerable ambiguity arises in determining which slope one should use in the comparison with theory. Furthermore, the resistance curves (particularly the dc data) often exhibit kinks near H_{c2}, which may or may not be related to the peak effect. In the face of such kinks, one group of experimenters took the slope at magnetic fields preceding the kink while another group took the slope past the kink. Such practices naturally lead to a wide scattering of data among different experimenters, as demonstrated in Fig. 1 which contains some 50 data points obtained at several different laboratories.

To circumvent these experimental difficutlies, in the present work we adopted the derivative technique which graphically displays the slope directly and permits extrapolation to H_{c2}. This technique enabled us to experimentally resolve the theoretical differences between Caroli and Maki, and Thompson. Our measurements were made at microwave frequencies to minimize the effects of pinning and Joule heating. High-concentration niobium-tanalum alloys ($Nb_{0.5}Ta_{0.5}$ and $Nb_{0.75}Ta_{0.25}$) were used since they are weak-coupled superconductors in the dirty limit as assumed in the theoretical treatments. In addition, measurements were made on low-concentration alloys ($Nb_{0.9}Ta_{0.1}$ and $Nb_{0.95}Ta_{0.05}$) to observe the departure from the dirty limit. We also measured three dirty lead-indium alloy samples ($Pb_{0.5}In_{0.5}$, $Pb_{0.83}In_{0.17}$, and $Pb_{0.9}In_{0.1}$) to note any effects resulting from the change to these strong-coupled superconductors. The particular composition of $Pb_{0.83}In_{0.17}$ was chosen in order to duplicate extensive measurements performed on this alloy in other laboratories.[8]

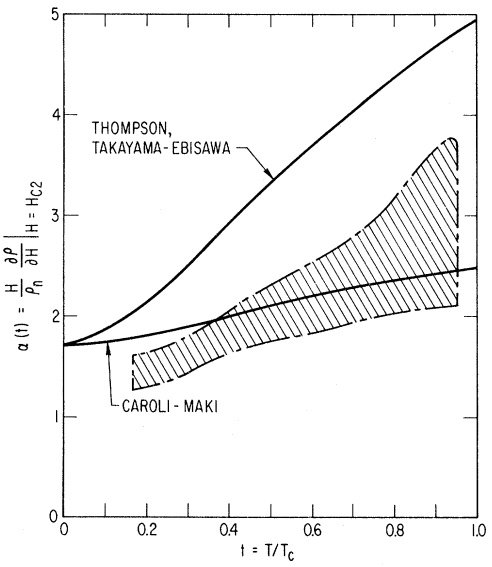

FIG. 1. Compilation of existing data for the slope of the flux-flow resistivity relevant to type-II superconductors of short mean free path. Some 50 data points are scattered within the shaded area. Reproduced from Fig. 9 of Ref. 6.

In Secs. II–IV we discuss the microscopic theory as applied to the surface resistance in the vortex state and then describe our apparatus and results in detail.

II. THEORETICAL RESPONSE TO ELECTRIC FIELDS

In this section we use the response functions calculated by Thompson to arrive at expressions for the dc flux-flow resistance and the microwave surface resistance. The difference between the Thompson and the Caroli–Maki theories is stated and reasons are given indicating why, although the former theory is correct in the immediate vicinity of H_{c2}, the latter theory may be correct in a region somewhat below H_{c2}.

First we recall certain parameters introduced by Maki[9] to describe the static vortex state. The first generalized Ginzburg–Landau κ parameter is

$$\kappa_1(t) = H_{c2}(t)/\sqrt{2}\,H_{cB}(t)\ ; \tag{1}$$

$t = T/T_{c0}$ is the temperature divided by the zero-field critical temperature; H_{cB} is the bulk thermodynamic critical field, which was calculated in the BCS theory; $H_{c2}(t)$ is obtained from the equation

$$\ln t = \psi(\tfrac{1}{2}) - \psi(\tfrac{1}{2}+\rho)\ , \tag{2}$$

where ψ is the digamma function; and $\rho = \epsilon_0/4\pi T$ and $\epsilon_0 = 2eDH_{c2}(t)$, where e is the magnitude of the electronic charge and D is the diffusion constant. (We let $\hbar = c = k_B = 1$.) The second generalized κ parameter is defined in terms of the slope of the magnetization M at H_{c2}:

$$4\pi\left(\frac{dM}{dH}\right)_{H_{c2}} = \{1.16\,[2\kappa_2^2(t)-1]+n\}^{-1}\ ; \tag{3}$$

n is the demagnetization coefficient, which equals 1 for our geometry of a thin disk perpendicular to the applied field.

The microwave response may be calculated in a

gauge where the scalar potential vanishes and the electric and magnetic fields are derivable from a time-dependent vector potential $A(t)=A_\omega e^{-i\omega t}$. The current j flowing in the superconductor is related to A by the response function Q, such that $j=-QA$. Since the electric field E is $-\partial A/\partial t$ we see that the conductivity σ equals $-Q/i\omega$.

Only the leading correction Q' to the normal-state response Q_n has been calculated near H_{c2}: $Q=Q_n+Q'$. The surface impedance Z then has the appearance of an expansion of the usual local-limit form[10]

$$Z=-\frac{4\pi i\omega}{(4\pi Q_n)^{1/2}}\left(1-\frac{Q'}{2Q_n}\right). \tag{4}$$

The surface resistance R is the real part of Z, i.e.,

$$R=R_n[1-(\mathrm{Im}Q'-\mathrm{Re}Q')/2\omega\sigma_n] \ , \tag{5}$$

where R_n and σ_n are the normal-state values of R and σ. The experimental data will be presented in terms of the normalized slope S of R near H_{c2}:

$$S=\frac{H_{c2}}{R_n}\left(\frac{\partial R}{\partial H}\right)_{H_{c2}} . \tag{6}$$

Expressions for Q' are found in Ref. 5. In the dc limit when $\omega\ll\pi(T_{c0}-T)$,

$$(\mathrm{Re}Q')/\omega=0 \ , \tag{7a}$$

$$(\mathrm{Im}Q')/\omega=4eM\,L_D(t)/8\pi T\rho \ , \tag{7b}$$

$$S=2\kappa_1^2(0)\,L_D(t)/\{1.16\,[2\kappa_2^2(t)-1]+n\} . \tag{7c}$$

The factor $L_D(t)$ is the only difference between the Thompson and the Caroli–Maki results in this limit. It varies smoothly from 1 at $T=0$ to 2 at T_{c0} and is expressed in terms of the first and second derivatives of the digamma function, ψ' and ψ'':

$$L_D(t)=2+\rho\,\psi''(\tfrac{1}{2}+\rho)/\psi'(\tfrac{1}{2}+\rho) . \tag{8}$$

In the region near T_{c0} where ω becomes comparable with $\pi(T_{c0}-T)$, the alternate expressions of Ref. 4 must be used, which require $\omega\ll\pi T_{c0}$ and $T_{c0}-T\ll T_{c0}$:

$$\mathrm{Re}Q'=-4eM\left(\frac{1}{2}\,\frac{\omega^2}{\omega^2+\epsilon_0^2}+\frac{\omega^2[1-2\rho\,\psi''(\frac{1}{2})/\psi'(\frac{1}{2})]}{4\epsilon_0^2+\omega^2}\right),$$

$$\mathrm{Im}Q'=2eM\omega\left(\frac{\epsilon_0}{\omega^2+\epsilon_0^2}+\frac{4\epsilon_0[1-2\rho\,\psi''(\frac{1}{2})/\psi'(\frac{1}{2})]}{4\epsilon_0^2+\omega^2}\right. \tag{9}$$

$$\left.+\frac{3\psi''(\frac{1}{2})}{4\pi T\psi'(\frac{1}{2})}\right).$$

Combining these expressions and replacing the arguments of the various ψ functions by $\frac{1}{2}+\rho$, which is allowed near T_{c0} since $\rho\ll\frac{1}{2}$ there, we obtain

$$S=\frac{2\kappa_1^2(0)}{1.16\,[2\kappa_2^2(t)-1]+n}\left\{x\left[\frac{x+1}{x^2+1}+\frac{4x+2}{4x^2+1}\right.\right.$$

$$\left.\left.\times\left(1-2\rho\,\frac{\psi''(\frac{1}{2}+\rho)}{\psi'(\frac{1}{2}+\rho)}\right)\right]+3\rho\,\frac{\psi''(\frac{1}{2}+\rho)}{\psi'(\frac{1}{2}+\rho)}\right\} , \tag{10}$$

where $x=\epsilon_0(t)/\omega$. Note that this formula is in fact good for the entire temperature range, since it reduces to Eq. (7c) for vanishingly small frequencies at all temperatures.

The above result for S is accurate only to zeroth order in $\omega/\epsilon_0(0)\approx\omega/\pi T_{c0}$. For the frequency 31.5 GHz and transition temperatures ≈ 6.85 K of our experiments this ratio $\omega/\epsilon_0(0)=\frac{1}{8}$. To be sure that the error in the above expression is less than $\frac{1}{8}$ and is not several times this ratio, we have gone back to Ref. 5 and reexpanded all the expressions for Q' keeping the next-order corrections accurately. The more complicated expression for S which results is

$$S=\frac{2\kappa_1^2(0)}{1.16\,[2\kappa_2^2(t)-1]+n}\left[x\left(\frac{1}{1+4x^2}+C+D\right)\right.$$

$$-\rho\,\frac{\psi''(\frac{1}{2}+\rho)}{\psi'(\frac{1}{2}+\rho)}\,(-A-B+C-D)$$

$$+\frac{\rho^2}{x}\,\frac{\psi'''(\frac{1}{2}+\rho)}{\psi'(\frac{1}{2}+\rho)}\,(-A+B+\tfrac{2}{3}C+\tfrac{2}{3}D)$$

$$\left.+\frac{2\rho\psi'(\frac{1}{2}+\rho)}{\psi(\frac{1}{2}+3\rho)-\psi(\frac{1}{2}+\rho)}\,\frac{4x^2(2x+1)}{(1+4x^2)^2}\right] , \tag{11}$$

with

$$A=1+\frac{1}{1+4x^2} \ , \quad B=\frac{2x}{1+4x^2} \ ,$$

$$C=\frac{x}{1+x^2}+\frac{16x^3}{(1+4x^2)^2} \ ,$$

$$D=\frac{1}{1+x^2}+\frac{1}{1+4x^2}-\frac{8x^2}{(1+4x^2)^2} \ ,$$

and $x=\epsilon_0(t)/\omega$ as before. The error in this expression is of order $[\omega/\epsilon_0(0)]^2=\frac{1}{64}$ for our experiments. The simpler expression [Eq. (10)] results in a value for S which deviates from the Eq. (11) calculation by a maximum of 7% for $\omega/\epsilon_0(0)=\frac{1}{8}$, which would be accurate enough for our purposes. However, we have evaluated the more accurate results using Eq. (11) for comparison with experiment. Equation (11) is plotted in Fig. 2 for various ratios of frequency to transition temperature.

Fischer *et al.*[8] used a solution for S derived from the Caroli–Maki approach and found a frequency correction in the form of a multiplying factor so that

$$S=\frac{2\kappa_1^2(0)}{1.16\,[2\kappa_2^2(t)-1]+n}\,\frac{1+y}{1+y^2} \ , \tag{12}$$

where $y=\omega/2\epsilon_0(t)$. We have also plotted this equation for various transition temperatures with our data in Sec. IV.

Finally, we wish to discuss the basic difference

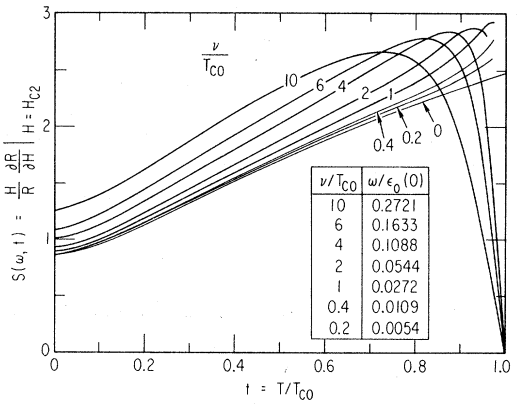

FIG. 2. Normalized slope $S(\omega, t)$ of the surface resistance at H_{c2} calculated from Eq. (11) of the text, assuming $2\kappa^2 \gg 0.16$. The parameter ν/T_{c0} is the ratio of the frequency in GHz to the zero-field transition temperature in K. The corresponding energy ratios $\omega/\epsilon_0(0)$ are listed.

between the Thompson and the Caroli–Maki theories in order to understand why they can have different regions of validity. As discussed in Ref. 5, the Caroli–Maki calculation includes only those parts of the response which are entirely "regular," consisting of products of only retarded or of only advanced Green's functions. The region of validity of expansions of these expressions in powers of the order parameter Δ is $\Delta \ll \pi T_{c0}$, the same as for static thermodynamic quantities. Expressed in terms of magnetic fields this restriction requires only that $1 - H/H_{c2}(t) \ll 1$, a reasonably large range.

The term Thompson found that Caroli and Maki had neglected is "anomalous," containing products of both retarded and advanced Green's functions. Such quantities arise only for dynamic quantities, like the conductivity, and have a much narrower range in which expansions in powers of the order parameter converge, requiring $\Delta \ll \epsilon_0(t)$ or, equivalently, $1 - H/H_{c2}(t) \ll H_{c2}(t)/H_{c2}(0) \approx 1 - t$.

Our experiments confirm Thompson's analysis in this very narrow region near H_{c2}. However, in the broader range where expansions of the anomalous terms in powers of Δ are not valid our experimental results tend to the Caroli–Maki results, indicating that the contribution of the anomalous terms is then apparently suppressed relative to the regular ones.

Exact calculations of the conductivity have not been made for this region. However, we can perform a heuristic comparison with another situation which has been well-understood theoretically, i.e., a superconductor containing a pair-breaking interaction such as with paramagnetic impurities but with a uniform Δ. For the comparison the actual effects of the magnetic field and the spatial variations of Δ are replaced by a pair-breaking interaction which gives the same shift of T_c from T_{c0}, and $|\Delta|^2$ is replaced everywhere by its spatially averaged value. In the $\omega \to 0$ limit, the leading contribution to the conductivity from the anomalous term Q_a' mentioned above gives for T near T_{c0}

$$\mathrm{Im}Q_a'/\omega = 4eM/2\epsilon_0 \qquad (13)$$

in the region $\Delta \ll \epsilon_0$ just as in Eq. (7b). This anomalous contribution just equals the leading regular contribution here, which accounts for the total in Eq. (7b) being twice the Caroli–Maki results near T_{c0}. In contrast, in the region $\epsilon_0 \ll \Delta \ll \pi T_{c0}$ one finds[11]

$$\mathrm{Im}Q_a'/\omega = 4eM(2/3\pi\Delta)\ln(16\Delta/\epsilon_0)\,. \qquad (14)$$

Since the regular term Q_r' is unchanged, the ratio is

$$\mathrm{Im}Q_a'/\mathrm{Im}Q_r' = (4\epsilon_0/3\pi\Delta)\ln(16\Delta/\epsilon_0)\,. \qquad (15)$$

This ratio tends to zero since $\epsilon_0 \ll \Delta$. If all anomalous contributions are similarly suppressed relative to the regular ones, then the Caroli–Maki expressions become correct.

We caution that this demonstration is not a rigorous proof. In fact, we run into divergence difficulties when we try to calculate corrections to the conductivity proportional to $\Delta(r) - \langle|\Delta|^2\rangle^{1/2}$, taking into account the spatial inhomogeneity. A similar heuristic model giving similar results has recently been proposed by Takayama and Maki.[12]

III. EXPERIMENTAL DETAILS

The surface resistance measurements were performed in the Andonian Dewar shown in Fig. 3. The Dewar was positioned so the microwave cavity in the Dewar tailpiece was centered between the pole pieces of a 12-in. magnet. This magnet was equipped with tapered pole pieces and modulation coils to provide dc field levels up to 15 kOe and modulation levels up to 80 Oe peak to peak. The temperature in the experimental chamber was varied by adjusting the throttle valve connection to the liquid-helium reservoir and controlling the power to the heater. With this arrangement, temperature could be varied between room temperature and approximately 2 K.

A. Microwave-Cavity Design

The samples were disks located in the center of the end plates of a right-circular-cylindrical cavity operating at 31.5 GHz in the TE_{011} mode. The cylindrical wall of the cavity had a diameter/length ratio of 2.09 and was machined with a groove 0.002 in. deep and 0.1 in. wide around its center. This groove lifted the degeneracy of the TM_{111} and the TE_{011} modes by about 0.15 GHz and was sufficient to prevent any effects of double moding from being observed.

The cavity was made of brass to minimize eddy-

current heating by the modulation field, and was silver plated approximately 0.003 in. thick to reduce microwave losses. Some end plates were made of oxygen-free high-conductivity (OFHC) copper without seriously affecting the lowest temperatures attainable.

A variable coupling network was used to optimize coupling for each sample run. The coupling was adjusted by changing the effective length of a cutoff waveguide section by varying the insertion of a dielectric plug. While this device was very convenient to use, it did introduce variable losses which made it difficult to make absolute measurements of surface resistivity. Since the main interest was in relative measurements (changes between the normal and superconducting state) this effect was not detrimental.

Samples were held in place in a shallow recess in the end plates with Apiezon type-N vacuum grease. A 0.410-in.-diam recess was used for the Nb-Ta samples, while a 0.600-in.-diam recess (the full inner diameter of the cavity) was used for the Pb-In samples.

B. Carbon-Resistor Thermometer

Two $\frac{1}{8}$-W Ohmite carbon resistors of nominal 270-Ω resistance were sealed in a 0.062-in.-diam hole in the cavity body with GE 7031 varnish for temperature measurement. One of the resistors was used to measure the temperature of all samples during the various runs. It was calibrated against the liquid-helium vapor pressure in the range 2–4.2 K and against a calibrated germanium thermometer in the 4–25 K range. The data were least-squares fit to a three-parameter logarithmic function so that

$$T=\frac{2.9718}{\log_{10}(R)+4.2377/\log_{10}(R)-4.1993} \quad . \tag{16}$$

In the range 2–15 K, the experimental points fit this equation to within ±30 mK.

Apparent temperature changes of approximately 10 mK, which were ignored, were produced by applied magnetic fields of 15 kOe or by absorbed rf powers of about 25 mW. In sample runs, the microwave power was restricted to convenient levels of less than about 4 mW.

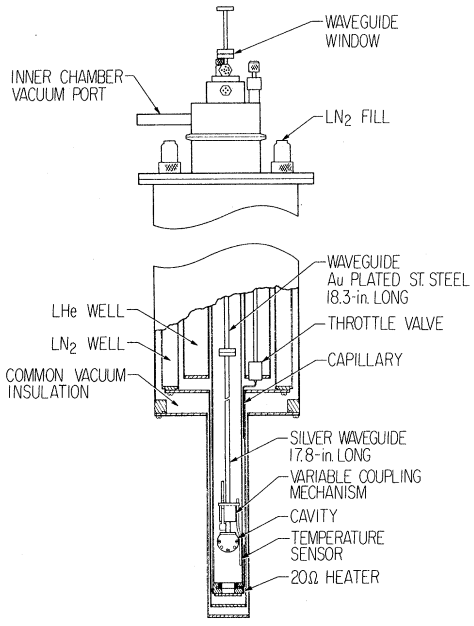

FIG. 3. Cross section of the variable-temperature Andonian Dewar used to cool the measurement apparatus to liquid-helium temperatures. The temperature of the superconducting sample mounted in the microwave cavity was measured by determining the resistance of a carbon resistor embedded in the cavity wall.

C. Microwave Circuitry

The microwave measuring circuit for obtaining derivative measurements of the cavity response is shown in Fig. 4. The output of the klystron is coupled into the sum arm of the magic T while the power reflected from the cavity is coupled out the difference arm into the crystal detector. The slide-screw tuner mounted on the fourth arm of the magic T is calibrated to present a mismatch which cancels the reflection of the waveguide window used to seal the waveguide entering the Dewar. The positions of the tuner and window are such that the calibration holds over a reasonably broad frequency band. The tuner was calibrated in 0.1-GHz increments and was found to vary only slightly within this range.

The crystal detector output was used to drive a klystron stabilizer to keep the klystron frequency centered on the cavity response and to drive an x-y recorder via the phase-lock detector. The x axis of the recorder was driven by the output of the rotating-coil gaussmeter and thus was provided with a voltage linearly proportional to the impressed dc magnetic field. This gaussmeter was calibrated against a nuclear-magnetic-resonance fluxmeter at the high-field settings.

A ten-turn pickup coil with mean diameter of 4.11 cm was taped to the center of one pole piece to measure the modulation amplitude. At 40 Hz the peak-to-peak modulation was 3 G per peak-to-peak mV.

In order to calibrate the recorded-crystal-detector modulation as a function of field, the dc output of the crystal detector was occasionally plotted versus field with zero modulation. The slope of this curve was then compared with the phase-lock detected modulation signal. The modulation drive was not constant with dc field owing to saturation ef-

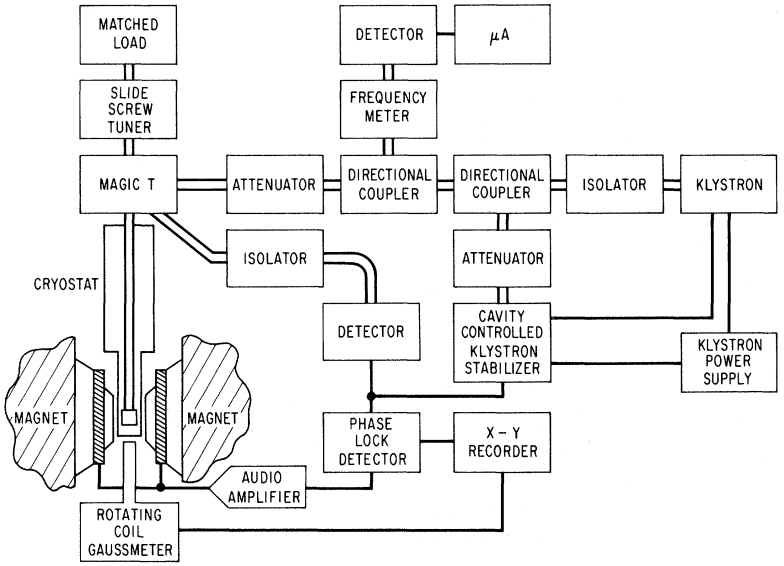

FIG. 4. Microwave measuring circuit for obtaining derivative measurements of the cavity response. The klystron frequency is locked to the resonance frequency of the helium-cooled microwave cavity and the phase-lock detector circuit measures the derivative of the sample surface resistivity. The rotating-coil gaussmeter provides a linear measure of the applied dc magnetic field.

fects of the magnet iron core, so periodic calibrations were also made of this quantity. The output of crystal detector was determined to be square law over our usual operating voltage range of 1–35 mV.

A plot such as that shown in Fig. 5 was made during each sample run to allow a determination of the relative power incident on the cavity at resonance. In a frequency range such that only one mode of the cavity is appreciably excited, the ratio of the reflected to the incident microwave power as a function of frequency is[13]

$$\frac{P_r(f)}{P_i(f)} = \frac{P_r(f_0)/P_i(f_0) + 4(f-f_0)^2/(\Delta f)^2}{1+4(f-f_0)^2/(\Delta f)^2} \quad , \tag{17}$$

where $P_r(f_0)/P_i(f_0)$ is the ratio at the resonant frequency f_0 and Δf is the half-width of the resonance. The incident power at several frequencies was determined by iteratively fitting the equation to the resonance curve.

In addition to the complete absorption curves displayed in Fig. 5, there are several partial curves displayed. These indicate the effect of the helium gas present inside the cavity due to the temperature-regulation system. The frequency shifts are in accord with those calculated from the Clausius–Mossotti[14] equation. The pressure was held relatively constant during a run to minimize the effect of these shifts.

D. Data Reduction

We represent the cavity as a simple R-L-C circuit in series with the waveguide impedance z_0. The loaded Q of this circuit is just

$$Q_L = \omega_0 L/(R+z_0) = Q_U/(1+z_0/R) \, , \tag{18}$$

where Q_U is the cavity unloaded Q. By definition, the Q of the coupling hole Q_n, representing radiated power loss from the cavity, is related to Q_U and Q_L by

$$1/Q_L = 1/Q_U + 1/Q_n \, . \tag{19}$$

Multiplying Eq. (19) through by Q_U and then comparing the results to Eq. (17), we find that

$$Q_U/Q_n = z_0/R \, , \tag{20}$$

or for the undercoupled case, $Q_n > Q_U$, Q_n/Q_U = $VSWR$ at resonance. Separating the sample surface resistance R_S from the rest of the cavity los-

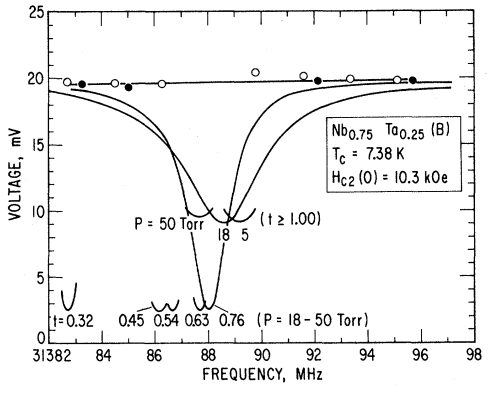

FIG. 5. Typical cavity response made using a tunable crystal-controlled klystron stabilizer. The partial resonance curves illustrate how the cavity frequency is affected by changes in the helium-gas pressure and temperature. The filled and open circles were derived from the normal and superconducting-state responses according to a procedure described in the text to determine the incident power level.

ses, represented by R_N, we can relate the losses to the reflection coefficient at resonance Γ by the relation

$$(R_N + BR_S)/A = (1+\Gamma)/(1-\Gamma)\,, \tag{21}$$

where A and B are geometric factors. By letting $\Gamma = \Gamma_0$ at low temperature and zero field when $R_S = 0$, and $\Gamma = \Gamma_N$ when $R_S = R_S(H_{c2})$ is the normal-state surface resistance, we can solve the resultant equations for the ratio

$$\frac{R_S(H)}{R_S(H_{c2})} = \frac{(\Gamma-\Gamma_0)(1-\Gamma_N)}{(1-\Gamma)(\Gamma_N-\Gamma_0)}\,. \tag{22}$$

Substituting $V^{1/2}/V_R^{1/2}$ for Γ and differentiating $R_S(H)/R_S(H_{c2})$ with respect to H, we get the final result

$$S(\omega, t) = \frac{H(V_R^{1/2} - V_0^{1/2})}{2V_N^{1/2}(V_N^{1/2} - V_0^{1/2})(V_R^{1/2} - V_N^{1/2})} \times \left(\frac{\partial V}{\partial H}\right)_{Hc2} \tag{23}$$

in terms of the various crystal detector voltages. Referring again to Fig. 5, V_0 is the voltage we measure in the resonance null at the lowest temperature reached and V_N is the voltage of the resonance null when the superconductor is in the normal state. V_R is the detector voltage corresponding to the input power to the cavity. We thus see that the quantity we record in our measurements, $\partial V/\partial H$, is directly proportional to the slope of the surface resistivity.

IV. EXPERIMENTAL RESULTS

We have made measurements of type-II superconductors in the vortex state with samples from three different type-II superconductor categories. Our main interest was on weak-coupled superconductors in the dirty limit since these conditions are assumed in the theoretical developments. The alloys of niobium and tantalum with niobium concentrations between 50 and 80 at.% fit in this category. Pure niobium is a clean-limit type-II superconductor while alloys with greater than 80% niobium are in a category between the dirty and clean limits. We have measured various alloy samples ranging from 50- to 95-at.% Nb.

Alloys of lead are, in contrast, strong-coupled type-II superconductors with the high-concentration alloys in the dirty-limit category. We include measurements on dirty-limit Pb-In alloys, that is, alloys with 10- to 50-at.% In.

A. Determination of T_{c0}, H_{c0}, and $\partial V/\partial H$ at H_{c2}

Figure 6 shows typical measurements which illustrate the advantages of the derivative technique. While most of our measurements were made with the applied magnetic field perpendicular to the sample, this figure shows the differences which

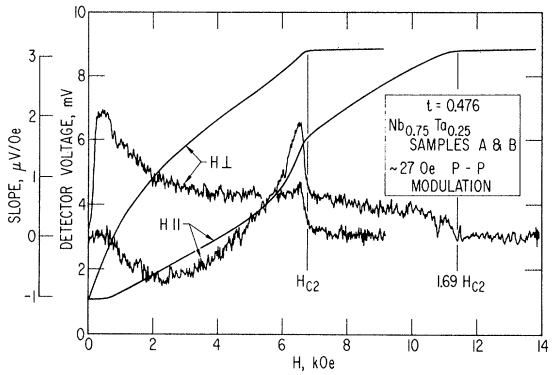

FIG. 6. Measurements to illustrate the differences in response between the magnetic field perpendicular and parallel to the sample surface. The smooth lines are recordings of the crystal-detector output vs field and the noisy curves are corresponding recordings using the derivative apparatus. P-P means peak to peak.

occur in parallel fields. The smooth curves in each case are the detector voltages versus field and the noisy curves are their derivatives. The relative ease in determining the slopes and transition fields from the derivative data at H_{c2} and H_{c3} ($= 1.69 H_{c2}$) is quite evident. (The derivative curves for the parallel-field case also illustrate an interesting phenomenon. Although the detector voltage increases monotonically with increasing field, the slope data starts out negative and then reverse near $H = 2$ kOe. The modulated signal was observed on an oscilloscope to make a smooth 180° phase reversal in the region 0.5–5.0 kOe. This observation was not pursued in detail.)

A plot of the slope data for a $Nb_{0.75}Ta_{0.25}$ sample is shown in Fig. 7. These data are typical of those obtained for all samples and will be used to illustrate the techniques used to obtain values for T_{c0}, H_{c2}, and $\partial V/\partial H$ at H_{c2} to evaluate S at H_{c2} from Eq. (23).

It will be observed that the slope at a constant temperature is a slowly varying function of the applied field H for moderate values of H. As the critical field is approached, the slope begins to increase almost linearly with the field and then rather abruptly it begins to decrease, again more or less linearly. Finally, at large fields the sample is normal and the slope is zero.

Instead of displaying a discontinuity in the slope at a well-defined transition field, the curves indicate a broad transition and thus present some difficulty in providing a comparison with theory. The broadening may be due partly to sample inhomogeneities, in addition to the unavoidable intrinsic thermodynamic fluctuation broadening. (The Nb-Ta samples were all annealed at 1800 °C for 2 h and then at 1900 °C in an attempt to reduce inhomogeneities.

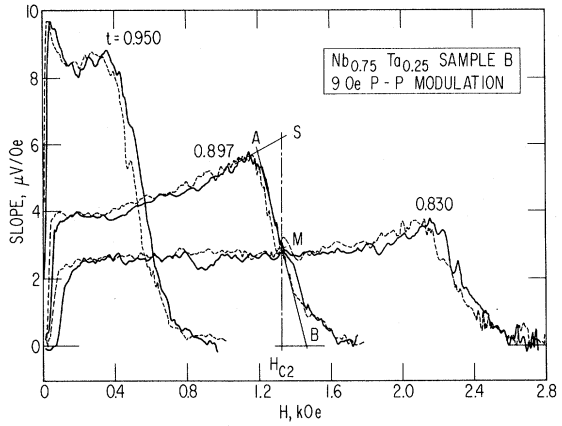

FIG. 7. Tracing of some of the recorded slope data for a $Nb_{0.75}Ta_{0.25}$ sample showing the construction used to obtain H_{c2} and the slope at H_{c2}. Lines A-B and A-S are drawn through the data and a perpendicular is erected intersecting A-B at its midpoint M. The coordinates of the point S are taken to be the values for H_{c2}. The solid lines are recordings made for the increasing field while the dashed lines are recordings obtained with the decreasing field.

The annealed samples did have a slightly narrower transition than unannealed samples.) In any case, a technique was devised for obtaining consistent repeatable values for T_{c0}, H_{c2}, and $\partial V/\partial H$ at H_{c2} from the data.

As seen in Fig. 7, the technique consisted in extending the linear portions of the slope-versus-field curves in and near the transition region. H_{c2} was then defined as the field at the midpoint of the decreasing H curve between the intersection with the increasing H curve and zero slope. The value of $\partial V/\partial H$ at H_{c2} was then obtained from the extended portion of the increasing H line at its intersection with $H = H_{c2}$. From the values of H_{c2} so obtained at various temperatures, a least-squares fit of H_{c2} vs T^2 was made and extrapolated to $H_{c2} = 0$ to obtain T_{c0}.

B. Nb-Ta Alloys

The data for the various Nb alloy samples are plotted in Fig. 8. There is a definite difference between the dirty-limit data ($Nb_{0.5}Ta_{0.5}$ and $Nb_{0.75}Ta_{0.05}$) and the clean-limit data ($Nb_{0.9}Ta_{0.1}$ and $Nb_{0.95}Ta_{0.05}$). The slope discontinuity for the dirty-limit samples is high but not quite as large as that calculated from Eq. (11). For comparison, we have plotted both the Thompson result [Eq. (11)] and the Fischer *et al.* modification of the Caroli-Maki theory [Eq. (12)]. In both of these expressions we have used the theoretical temperature variation of κ_2 as calculated by Caroli *et al.*[15]

We have included two sets of measurements of $Nb_{0.5}Ta_{0.5}$ samples. In one case, the measurements were made while two similar samples were mounted in the cavity, one on each end wall. In the other and more usual case, only one superconducting sample was used. The two sets of data are in good agreement and illustrate the repeatability of the measurements.

Within the accuracy of our measurements, the slope in the vicinity of the H_{c2} transition varied linearly with field. This provides some justification for our technique for reducing the data. If we choose to use the generally constant slope some distance below the transition, the data fall in the vicinity of the Caroli-Maki curves.

C. Slope Measurements of Dirty Pb-In Alloys

Our measurements of dirty Pb-In alloys follow closely the theoretical curves of Thompson as shown in Fig. 9. Thus, the present measurements do not support the evidence for a possible strong-coupling effect for the Pb-In alloys as suggested by the analysis of Fischer *et al.*[8] Just as in the case of the weak-coupling Nb-Ta alloys, we can also obtain low values of $S(\omega, t)$ near the Caroli-Maki curve by choosing slopes in the more constant slope region of the transition curves. We have included measurements on a $Pb_{0.83}In_{0.17}$ sample for comparison with the extensive data of Fischer *et al.*[8] for a similar sample; in general, our values for $S(\omega, t)$ are about 20% higher than their values.

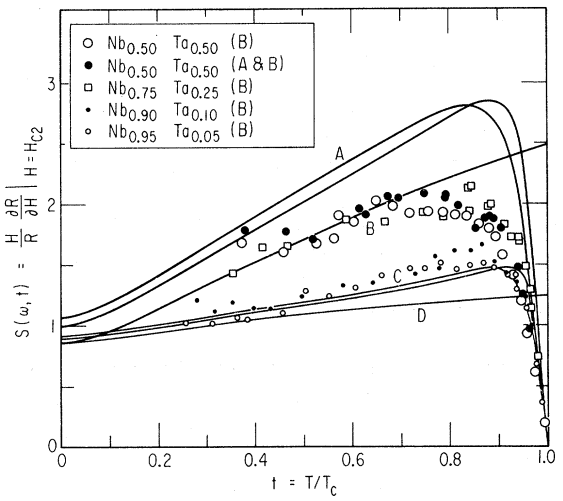

FIG. 8. Slope data for the various Nb-Ta alloys are plotted against various theoretical curves. The dirty-limit samples (with Ta concentrations greater than 20%) have larger slopes than the cleaner samples. The theoretical curves are all based on dirty-limit theory. The A curves are based on Thompson's calculations [Eq. (11)] with the experimental parameters 31.4 GHz and the transition temperature extremes 5.8 and 8.5 K. Curve B is also based on Eq. (11) but in the low-frequency limit $\omega \to 0$. Curves C and D are similar but are based on the calculation of Fischer *et al.* [Eq. (12)].

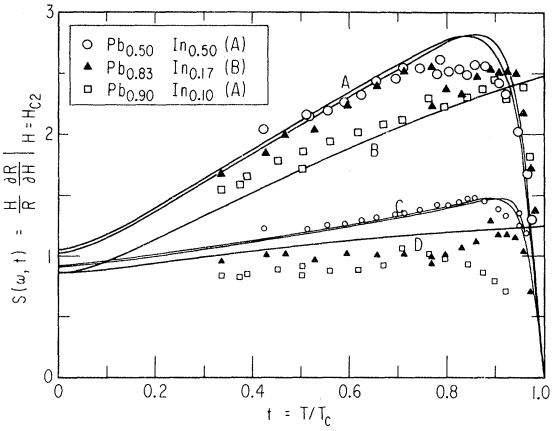

FIG. 9. Slope data for the Pb-In alloys plotted against the same theoretical curves described in Fig. 8. The transition-temperature extremes used in the calculations of curves A and C are 6.2 and 7.0 K, corresponding to the Pb-In data. In addition, data from the regions of relatively constant slope somewhat below H_{c2} are indicated by the smaller symbols.

D. Discussion of Results

Comparison of the slope data with theory is complicated by the lack of a sharp transition at a well-defined H_{c2}, as well as by the observation that the slope begins to increase with field just before the transition region. If this change in slope is ignored and the relatively constant value some distance below H_{c2} is used for comparison with theory, the results compare favorably with the Caroli–Maki theory. On the other hand, extrapolating the changing slope to H_{c2} as described earlier provides results which compare well with the dirty-limit theory of Thompson. An explanation for this behavior is contained in Sec. II where it is pointed out that the Thompson correction is valid only near H_{c2} and the Caroli–Maki result may be accurate for a range of fields somewhat below H_{c2}.

V. CONCLUSION

Measurements of the derivative of the normalized surface resistance of samples of dirty type-II superconductors with respect to the magnetic field compare favorably with the theoretical predictions of Thompson and Takayama and Ebisawa, when the measured values of the derivative are extrapolated to H_{c2}.

If the derivative is obtained from the region below the transition where its value is relatively constant, results which support the Caroli–Maki theory are obtained. Data collected without the benefit of the derivative technique would tend to yield such results. However, the data obtained by an appropriate extrapolation in the immediate vicinity of H_{c2} support the Thompson correction to the Caroli–Maki theory.

ACKNOWLEDGMENTS

One of the authors (R. J. P.) would like to thank Frank Vernon for his continued encouragement and for some helpful discussions. The assistance of Todd Smith in the preparation of the manuscript is gratefully acknowledged.

*Based in part on a Ph.D. thesis submitted by R. J. Pedersen to the U.S.C. Graduate School (August, 1971). Work at U.S.C. supported by the National Science Foundation and the U.S. Atomic Energy Commission.

[1]A. Schmid, Phys. Kondens. Mater. **5**, 302 (1966).

[2]Y. B. Kim, C. F. Hempstead, and A. R. Strand, Phys. Rev. **139**, A1163 (1965); A. R. Strand, C. F. Hempstead, and Y. B. Kim, Phys. Rev. Lett. **13**, 794 (1964).

[3]C. Caroli and K. Maki, Phys. Rev. **164**, 591 (1967).

[4]C. Caroli and K. Maki, Phys. Rev. **159**, 306 (1967).

[5]R. S. Thompson, Phys. Rev. B **1**, 327 (1970).

[6]H. Takayama and H. Ebisawa, Prog. Theor. Phys. **44**, 1450 (1970).

[7]Y. B. Kim, *Proceedings of the Twelfth International Conference on Low Temperature Physics, Kyoto, Japan,* edited by E. Kanada (Academic Press of Japan, Tokyo, 1971), p. 231.

[8]G. Fischer, R. D. McConnell, P. Monceau, and K. Maki, Phys. Rev. B **1**, 2134 (1970); Phys. Rev. B **2**, 2817 (1970).

[9]K. Maki, Physics (N.Y.) **1**, 21 (1964).

[10]R. S. Thompson, Phys. Rev. B **3**, 1617 (1971).

[11]Yu. N. Ovchinnikov, Zh. Eksperim. i Teor. Fiz. **59**, 128 (1970) [Sov. Phys.-JETP 32, 72 (1971)]. See the expressions for Im Q' in Eqs. (47) and (50), substituting $\Gamma = 1/2\epsilon_0$.

[12]H. Takayama and K. Maki, Phys. Rev. Lett. **28**, 1445 (1972).

[13]J. C. Slater, *Microwave Electronics* (Dover, New York, 1969).

[14]WADD Tech. Rept. No. 60-56, July, 1960, edited by V. J. Johnson, p. 7.001 (unpublished).

[15]C. Caroli, M. Cyrot, and P. G. deGennes, Solid State Commun. **4**, 17 (1966).